Applied Physics Express

LETTER • **OPEN ACCESS**

Coherent X-ray diffraction of the M_1 to M_2 structural phase transition in a single vanadium dioxide nanocrystal

To cite this article: Marcus Newton *et al* 2022 *Appl. Phys. Express* **15** 077001

OPEN ACCESS

Applied Physics Express 15, 077001 (2022) LETTER

https://doi.org/10.35848/1882-0786/ac7777

Coherent X-ray diffraction of the M_1 to M_2 structural phase transition in a single vanadium dioxide nanocrystal

Marcus Newton[1*], Ulrich Wagner[2], and Christoph Rau[2]

[1]Department of Physics & Astronomy, University of Southampton, United Kingdom
[2]Diamond Light Source, Harwell Oxford Campus, Didcot, United Kingdom

*E-mail: M.C.Newton@soton.ac.uk

Received May 17, 2022; revised May 31, 2022; accepted June 8, 2022; published online June 20, 2022

Correlated electronic materials are of interest due to strong coupling between lattice, spin and orbital degrees of freedom that give rise to emergent behaviour that is often of considerable utility for next-generation technologies. Vanadium dioxide is a prototypical material that undergoes a number of structural phase transitions near room temperature. Here are presented the results of coherent X-ray diffraction measurements on a single vanadium dioxide nanocrystal approximately 440 nm in size. Experimental findings are compared with ab-initio simulations to elucidate the origin of distortions that are observed in the diffraction pattern. © 2022 The Author(s). Published on behalf of The Japan Society of Applied Physics by IOP Publishing Ltd

Correlated electronic materials are those which the interaction between valence electrons can strongly influence the properties of the material.[1–4] They are interesting as their unique properties are of considerable utility for device physics, functional materials and furthering understanding of fundamental condensed matter physics. Many of these materials exhibit a displacive or reconstructive structural phase transformation (SPT) at some critical temperature T_c.

Vanadium dioxide (VO_2) is particularly interesting as it exhibits a number of SPT's including an ultra-fast SPT at a critical temperature of $T_c \sim 67$ °C in which VO_2 transforms to tetragonal lattice with space group $P4_2/mnm$. This is also accompanied by an ultra-fast femto-second metal-to-insulator transition (MIT) which is of considerable interest for next-generation devices such as ultra-fast all-optical switches that operate on the femto-second timescale.[5–9]

Cooling VO_2 from the high-temperature rutile phase to a temperature below T_c results in alternation of zigzag rotated and dimerised vanadium atoms chains along the rutile *c*-axis and a corresponding splitting of the $d_{||}$ band into bonding and anti-bonding states. In addition, the remaining π^* states are shifted above the Fermi level resulting in an electronic band gap of 0.7 eV. Alternate distortions of vanadium atoms chains along the rutile *c*-axis also result in an approximately doubled unit cell along the *b*-axis direction [Fig. 1(b)] and the emergence of a monoclinic (M_2) structure with space group C2/m. Further cooling from the M_2 phase toward ambient temperatures results in a continuous dimerisation of the zigzag chains while chains previously dimerised in the M_2 phase are gradually rotated (the triclinic phase). The M_1 phase is reached when both chain types are identically dimierised and rotated [Fig. 1(b)]. The resulting lattice structure has space group $P2_1/c$ and is approximately halved along the *b*-axis direction relative to the M_2 phase.[10,11]

In order to realise the aforementioned technological applications for VO_2, it is essential to understand its physical properties at the nanoscale during the SPT. Here we report on Bragg coherent X-ray diffraction of the M_1 to M_2 SPT in a single VO_2 nanocrystal. Coherent diffraction imaging (CDI) performed in the Bragg geometry enables probing of crystalline material structure in three-dimensions with sub-nanometre sensitivity. It is performed by illuminating a crystal with a spatially coherent X-ray source so that the coherence length exceeds the dimensions of the crystal. The resulting scattered light produces a three-dimensional interference pattern that encodes the atomic positions of atoms within the crystal. Computational techniques are then used to reconstruct the real-space object.[12–16]

VO_2 nanocrystals were synthesised in bulk on *c*-plane sapphire substrates using a thermal CVD method. A cleaned sapphire substrate was placed into a barrel furnace along side a crucible of VO_2 powder. The furnace was subsequently heated to 700 °C under high vacuum with a partial pressure of argon gas flowing at a rate between 1 and 5 sccm. The growth substrates were then inspected with optical microscopy and micro-manipulation used to transfer a single VO_2 nanocrystal to a clean silicon (100) substrate for synchrotron experiments.

Experiments were performed at the Diamond Light Source Coherence branch of beamline I13 (I13-1). A double crystal Si (111) monochromator was used to produce a beam of 8.877 keV, which corresponded to the minimum gap of the undulator to ensure a high brilliance beam. The beam was then focused using a Fresnel zone plate onto the sample mounted on a heated stage positioned at the eucentric point of the goniometer. The sample was rotated to locate the (011) reflection and diffraction data acquired using a Medipix3 Merlin detector mounted in the reflection geometry at a suitable distance to ensure sufficient oversampling. Measurements were taken at a range of temperatures from a single isolated VO_2 nanocrystal.

Figure 2(a) shows two-dimensional projections of the diffraction pattern of a single VO_2 nanocrystal at a range of temperatures during the SPT from M_1 to M_2 and finally to the rutile phase. Below 64 °C distortions are clearly visible around the centroid of the diffraction pattern and can be attributed to the gradual and spatially distributed transformation from the M_1 to M_2 phase. Distortions increase progressively as the nanocrystal is heated. In addition, asymmetry in the diffraction pattern indicates the presence of strain arising during the SPT due to differences in the lattice constants at domain boundaries as M_2 phases nucleate and grow within the

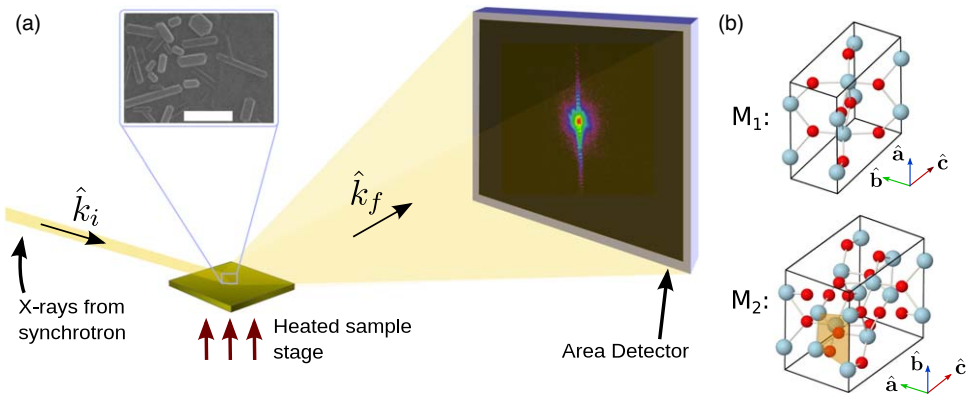

Fig. 1. (Color online) (a), Bragg CDI experimental geometry showing the incident ($\mathbf{k}_i$) and reflected ($\mathbf{k}_f$ X-ray wavevectors. Inset shows an electron micrograph of VO_2 nanocrystals as grown. (b), Unit cell structure for the M_1 and M_2 phases of VO_2. Larger blue spheres represent vanadium atoms while smaller red spheres represent oxygen atoms.

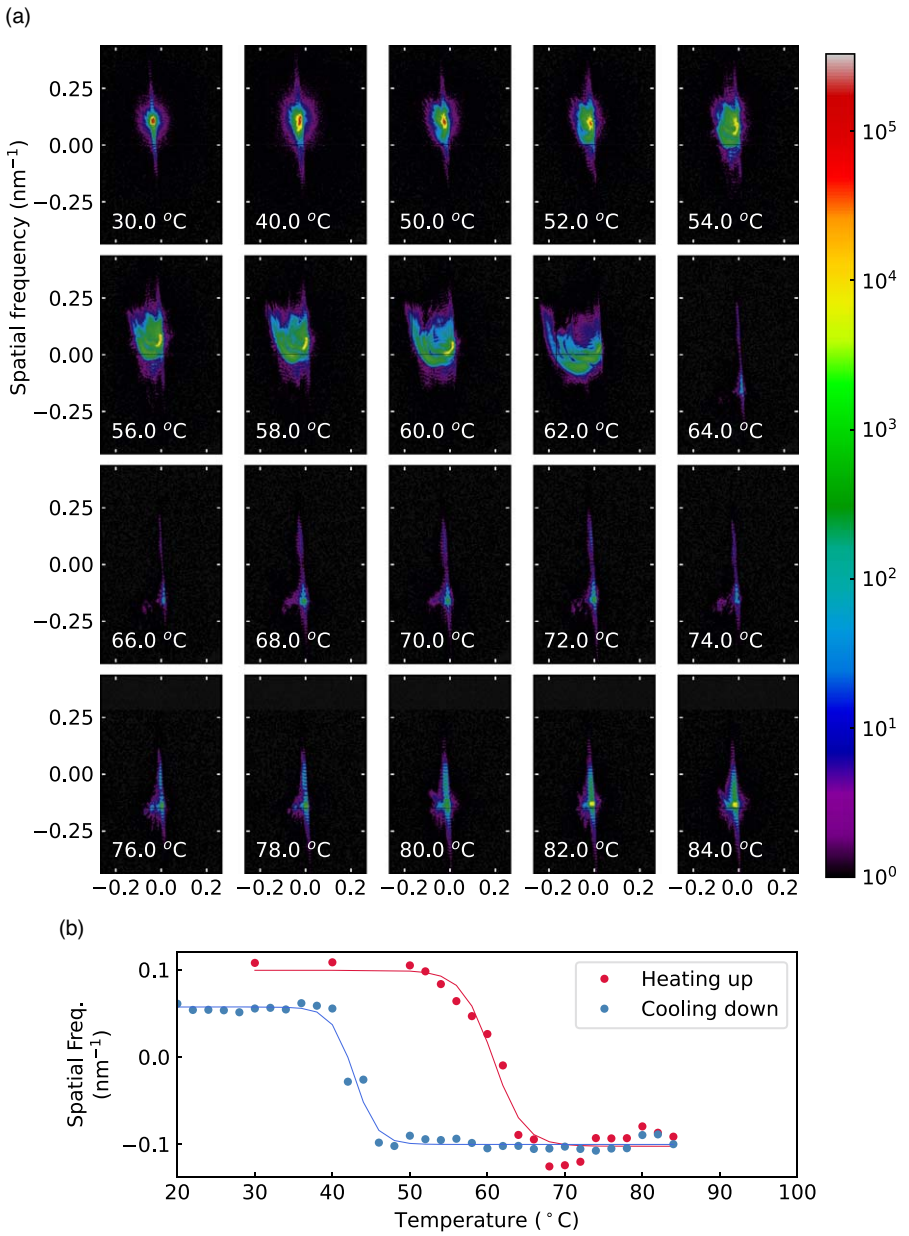

Fig. 2. (Color online) (a), Two-dimensional projection of coherent diffraction patterns of a single VO_2 nanocrystal at a range of temperatures. Distortions due to the SPT from M_1 to M_2 phase manifest with increasing temperature up to the rutile phase transition. (b), Hysteresis loop associated with the SPT of the diffraction speckle patterns centroid position.

nanocrystal.[17–19] Upon reaching a temperature of 64 °C, the distorted diffraction pattern centroid disappears and a new centroid spontaneously appears below. The centroid position remains largely unchanged with a further increase in temperature. This is attributed to the appearance of the (110) reflection of the high-temperature rutile phase which has a larger lattice spacing and hence a lower Bragg angle. Moreover, the difference in angle agrees well with the expected down shift in centroid elevation. Although there are reports that have observed a transition from the M_1 phase directly to the rutile phase,[20] this was not always observed in our samples where the M_2 phase was more commonly observed. This is likely due to external strain induced by defects during growth on the lattice-mismatched substrate or during mechanical micro-manipulation.

Upon cooling, the original diffraction pattern was recovered with a hysteresis of approximately 20 °C. Figure 2(b) shows the hysteresis loop associated with vertical displacement of the diffraction speckle patterns centroid position. Immediately after cooling to 20 °C, the centroid position was found to remain approximately $0.04\,\mathrm{nm}^{-1}$ below the initial spatial frequency. This likely occurred due to an incomplete transformation of the nanocrystal from the rutile phase back to the M_1 phase leaving some regions remaining in the rutile phase.[18]

As is often the case with materials that show strong phase structure, phase reconstruction of the real-space image via iterative and machine-learned phase retrieval has proven challenging due to strong distortions of the speckle pattern. We can instead gain insight into the SPT indirectly by comparison with atomistic simulated diffraction patterns. Our simulations employ a first principles approach as outlined in Ref. 21. Briefly, to simulate the M_1 to M_2 SPT, the summation over each unit cell is instead replaced with a summation over groups of unit cells (or supercells) of a fixed size that are adjacent within the crystal. The supercell size was chosen to remain below the resolution of the BCDI simulation, as required by the simulation constraints. Mosaic texture was then applied to one-half of the nanocrystal (divided along lattice vector directions normal to the **c**-axis direction, in the M_1 phase) via a random variation to an order parameter $t \in [0, t_{\max}]$ that defines the stage along the SPT transition trajectory for each supercell in the structure. So, when $t = 0$, the nanocrystal has M_1 structure and when $t = 1$ the nanocrystal has M_2. The remaining half of the crystal was fixed in the M_1 phase in order to induce strain at the interface between the two phases and hence asymmetry in the resulting diffraction pattern. Wyckoff internal coordinates for the $P2_1/c$ lattice structure are given by (x, y, z), $\left(-x, y+\frac{1}{2}, -z+\frac{1}{2}\right)$, $(-x, -y, -z)$ and $(x, -y+\frac{1}{2}, z+\frac{1}{2})$, where x, y and z are the fractional units. Wyckoff fractional units for VO_2 were taken from Eyert and shown in Table I.[10] Anti-dimerisation of alternative vanadium atom pairs was parametrised with a Wyckoff displacement of $\pm\left(\frac{1}{3}-x\right)t$ along the direction of lattice vector **a** while rotations were parameterised by $\mp(1-y)t$ along the direction of lattice vector **b**, in the M_1 phase notation. The scattering amplitude equation is given by:

$$A(\mathbf{q}) = \frac{r_0\sqrt{\Phi_0}}{R}\prod_i d_i \sum_{\mathbf{R}_{nd}}\sum_{\mathbf{r}_m} f_m(q)\, e^{-i\mathbf{q}\cdot(\mathbf{R}^m_{dn}+\tilde{\mathbf{u}}_m(\mathbf{R}_{nd}))}, \qquad (1)$$

Table I. Fractional coordinates for VO_2 in the M_1 phase.

Atom	Wyckoff positions	Parameters		
		x	y	z
V	(4e)	0.242	0.975	0.025
O_1	(4e)	0.10	0.21	0.20
O_2	(4e)	0.39	0.69	0.29

where the supercell lattice vector $\mathbf{R}^m_{nd} = \mathbf{R}_{nd} + \mathbf{r}_m$ and $\mathbf{R}_{nd} = n_1 d_1 \mathbf{a}_1 + n_2 d_2 \mathbf{a}_2 + n_3 d_3 \mathbf{a}_3$, n_i are positive integers, $\mathbf{r}_m$ are displacements of atom m within each unit cell, d_i are positive constant integer values for each index i and $\tilde{\mathbf{u}}_m$ is the average displacement of atom m in the supercell at position $\mathbf{R}_{nd}$.[21]

Figure 3(a) shows the resulting diffraction patterns for the (011) reflection of a single VO_2 nanocrystal of comparable size (approximately $440 \times 440 \times 44$ nm^3), as determined by the diffraction pattern fringe spacing in Fig. 2(a) at 30 °C. Simulated experimental parameters are equivalent to those of the synchrotron experiment with the exception of the detector size which was reduced to 256×256 pixels as this was found to be sufficiently optimal. Lattice parameters used for VO_2 in the M_1 phase are $a = 0.575$, $b = 0.453$, $c = 0.538$ and $\beta = 122.615$ °C. The oversampling ratio was fixed to 1.2 while the detector exposure time was set to 100 s.

Mosaic structure was incorporated by randomly assigning an order parameter value, with normal distribution, to each supercell, which consisted of 10^3 adjacent unit cells. Similar results were obtained when the supercell size was varied between 5^3 and 50^3 adjacent unit cells. The maximum value of the order parameter $t_{\max} \in [0, 1]$ is shown inset in each image of Fig. 3(a). As $t_{\max}$ is increased, the range of possible values of t increases and the nanocrystal becomes less ordered. This results in a significant broadening of the diffraction pattern toward the centroid region. Two-dimensional slices of the three-dimensional diffraction patterns through the centroid also clearly reveal broadening of the diffraction pattern toward the centroid region, as was observed experimentally.

Three-dimensional iso-surface images [Fig. 3(b)] clearly show that a broadening of the fringe pattern along the rocking curve direction is apparent and increases with increasing $t_{\max}$. It is also clear that the broadening only occurs along a single direction and can be understood as the transition from M_1 to M_2 is in part due to expansion and rotation of vanadium atom pairs predominantly about the b-axis direction, in agreement with experimental observation.

Figure 4 shows the χ^2 error plotted for both experimental coherent diffraction patterns (Fig. 2) and simulated coherent diffraction patterns (Fig. 3) using $\chi^2_i = \sum_{\mathbf{q}}(\sqrt{I_i(\mathbf{q})} - \sqrt{I_0(\mathbf{q})})^2 \big/ \sum_{\mathbf{q}} I_0(q)$, where I_0 is the initial diffraction pattern intensity, I_i the diffraction pattern intensity at either a given temperature or order parameter ($t_{\max}$) respectively and **q** is the spatial frequency. In both cases, an initial rapid increase in χ^2 is observed followed by an oscillatory decline. The simulated data shows overall lower values in χ^2 likely due to the presence of fewer phase domains than observed in the experimental diffraction patterns. Oscillations in χ^2 are however observed in both

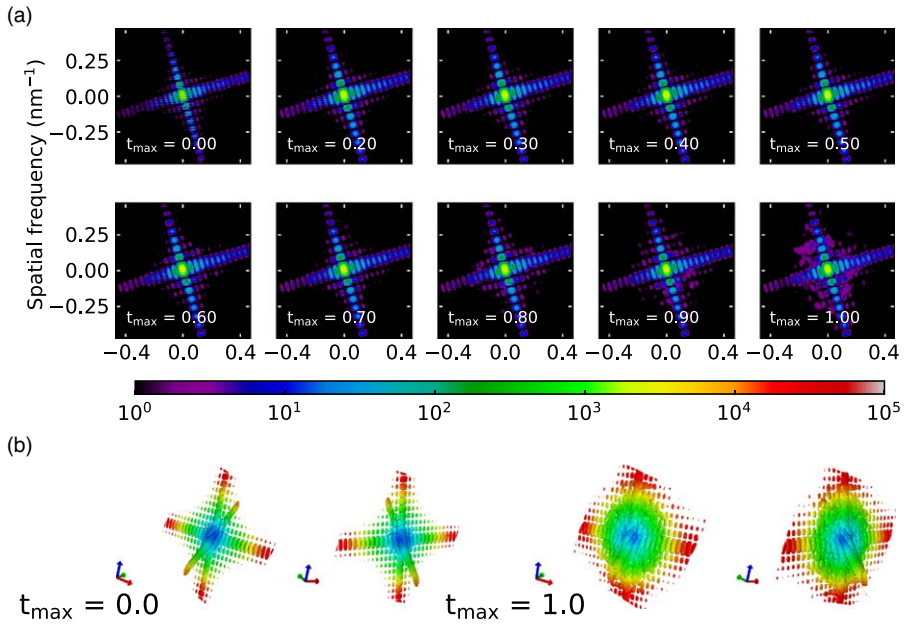

Fig. 3. (Color online) (a), Two-dimensional project of simulated coherent diffraction patterns of a single VO_2 nanocrystal undergoing the M_1 to M_2 SPT. (b), Three-dimensional iso-surface images of the diffraction patterns for $t_{max} = 0.0$ and $t_{max} = 1.0$.

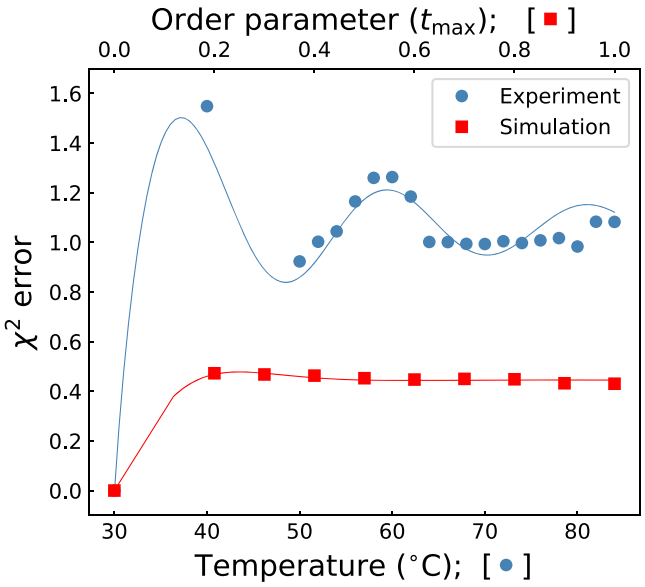

Fig. 4. (Color online) χ^2 error plotted for both experimental coherent diffraction patterns (Fig. 2) and simulated coherent diffraction patterns (Fig. 3).

cases, albeit less pronounced in the simulation, and are likely due to increasing asymmetry in the diffraction pattern.

In summary, we have imaged diffraction patterns from a single VO_2 nanocrystal undergoing a structural phase transition from the M_1 to M_2 phase. Our findings reveal the origin of broadening present in the diffraction pattern through comparison with complementary ab-initio simulations that are in good agreement. Differences in the observed diffraction and simulation are likely due to differing arrangements of M_1 and M_2 domain regions. A more complete description to include dynamical scattering effects will likely further improve the agreement between experiment and simulation and will likely form the topic of future studies. Our findings will also facilitate in further understanding the structural phase transition in VO_2 and efforts to recover three-dimensional images from nanocrystals that display strong phase structure.

Acknowledgments

We acknowledge Diamond Light Source for time on Beamline I13-1 under Proposal MT12587. We also acknowledge use of the IRIDIS High Performance Computing Facility, and associated support services at the University of Southampton, in the completion of this work.This work was supported by UK Research and Innovation (UKRI) grant MR/T019638/1 for the University of Southampton Department of Physics & Astronomy.

1) P. W. Anderson, "More is different," Science **177**, 393 (1972).
2) D. N. Basov, R. D. Averitt, D. van der Marel, M. Dressel, and K. Haule, "Electrodynamics of correlated electron materials," Rev. Mod. Phys. **83**, 471 (2011).
3) E. Dagotto, "Complexity in strongly correlated electronic systems," Science **309**, 257 (2005).
4) J. Quintanilla and C. Hooley, "The strong-correlations puzzle," Phys. World **22**, 32 (2009).
5) S.-H. Bae, S. Lee, H. Koo, L. Lin, B. H. Jo, C. Park, and Z. L. Wang, "The memristive properties of a single vo$_2$ nanowire with switching controlled by self-heating," Adv. Mater. **25**, 5098 (2013).
6) A. Cavalleri, C. Tóth, C. W. Siders, J. A. Squier, F. Ráksi, P. Forget, and J. C. Kieffer, "Femtosecond structural dynamics in VO_2 during an ultrafast solid-solid phase transition," Phys. Rev. Lett. **87**, 237401 (2001).
7) K. Liu, S. Lee, S. Yang, O. Delaire, and J. Wu, "Recent progresses on physics and applications of vanadium dioxide," Mater. Today **21**, 875 (2018).
8) M. Nakano, K. Shibuya, D. Okuyama, T. Hatano, S. Ono, M. Kawasaki, Y. Iwasa, and Y. Tokura, "Collective bulk carrier delocalization driven by electrostatic surface charge accumulation," Nature **487**, 459 (2012).
9) A. Zylbersztejn and N. F. Mott, "Metal-insulator transition in vanadium dioxide," Phys. Rev. B **11**, 4383 (1975).
10) V. Eyert, "The metal-insulator transitions of VO_2: a band theoretical approach," Ann. Phys. **11**, 650 (2002).
11) M. Hada, K. Okimura, and J. Matsuo, "Characterization of structural dynamics of VO_2 thin film on $c-Al_2O_3$ using in-air time-resolved X-ray diffraction," Phys. Rev. B **82**, 153401 (2010).
12) J. Miao, J. Kirz, and D. Sayre, "The oversampling phasing method," Acta Crystallogr. D **56**, 1312 (2000).

13) M. C. Newton, S. J. Leake, R. Harder, and I. K. Robinson, "Three-dimensional imaging of strain in a single ZnO nanorod," Nat. Mater. **9**, 120 (2010).
14) M. A. Pfeifer, G. J. Williams, I. A. Vartanyants, R. Harder, and I. K. Robinson, "Three-dimensional mapping of a deformation field inside a nanocrystal," Nature **442**, 63 (2006).
15) I. K. Robinson and J. W. Miao, "Three-dimensional coherent X-ray diffraction microscopy," MRS Bull. **29**, 177 (2004).
16) M. von Laue, "Dieäußere Form der Kristalle in ihrem Einfluß auf die Interferenzerscheinungen an Raumgittern," Ann. Phys. **26**, 55 (1936).
17) J. Cao et al., "Strain engineering and one-dimensional organization of metal–insulator domains in single-crystal vanadium dioxide beams," Nat. Nanotechnol. **4**, 732 (2009).
18) J. Jeong, N. Aetukuri, T. Graf, T. D. Schladt, M. G. Samant, and S. S. P. Parkin, "Suppression of metal-insulator transition in VO_2 by electric field-induced oxygen vacancy formation," Science **339**, 1402 (2013).
19) I. K. Robinson and I. A. Vartanyants, "Use of coherent X-ray diffraction to map strain fields in nanocrystals. proceedings of the international workshop on nanomaterials," Appl. Surf. Sci. **182**, 186 (2001).
20) J. H. Park, J. M. Coy, T. Serkan Kasirga, C. Huang, Z. Fei, S. Hunter, and D. H. Cobden, "Measurement of a solid-state triple point at the metal–insulator transition in VO_2," Nature **500**, 431 (2013).
21) A. H. Mokhtar, D. Serban, and M. C. Newton, "Simulation of Bragg coherent diffraction imaging," J. Phys. Commun. **6**, 055003 (2022).